ARPHA Preprints

PENSOFT

PREPRINT

Author-formatted, not peer-reviewed document posted on 16/12/2025

DOI: https://doi.org/10.3897/arphapreprints.e182608

Regional impact risk classification (RIRC): a predictive framework for plant invasion impacts

Mostafa Oveisi, Zahra Hazrati, Yan Sun, Mina Hejazi, Sven Bacher, Heinz Müller-Schärer

Regional impact risk classification (RIRC): a predictive framework for plant invasion impacts

Mostafa Oveisi[1*], Zahra Hazrati[1], Yan Sun[2], Mina Hejazi[3], Sven Bacher[4], Heinz Mueller Schaerer[1,2,4*]

[1] Department of Agronomy and Plant Breeding, College of Agriculture and Natural Resources, University of Tehran, Karaj, Iran

[2] College of Resources and Environment, Huazhong Agricultural University, Wuhan, China

[3] Department of Plant Protection, College of Agriculture and Natural Resources, University of Tehran, Karaj, Iran

[4] Department of Biology, University of Fribourg, Fribourg, Switzerland

[*] Corresponding email: moveisi@ut.ac.ir; heinz.mueller@unifr.ch

Abstract

Regional prediction of impact risk is essential for prioritizing targeted management of invasive alien plants. We present the Regional Impact Risk Classification (RIRC) framework, which combines the Environmental Impact Classification for Alien Taxa (EICAT) with species distribution models (SDMs) to connect ecological impact severity with the spatial likelihood of establishment and spread under current and future climates. Applying RIRC to 20 alien plants in Iran, we produced species-specific and aggregated regional maps, along with detailed climatic suitability projections. The analysis revealed significant regional contrasts: very high to extreme risks for salt- and drought-tolerant taxa along the southern coasts, a dominance of tree invaders in the southwestern lowlands and the Zagros, and hotspots of trees, woody climbers, and aquatic species in the northern provinces. Aggregated maps identified the Caspian coast and southern regions as hotspots for invasion risk. Under RCP 4.5 and 8.5 climate scenarios, RIRC levels increase along the northern and southern coasts but decline in central deserts, with species-specific responses ranging from strong expansions (e.g., *Cynanchum acutum*) to projected contractions (e.g., *Paulownia fortunei*). By linking impact severity with spatial dynamics, RIRC provides a scalable decision-support framework for guiding invasion management and conservation planning under current and future climates.

Keywords: climate suitability; EICAT; Invasive alien plants; Impact assessment, Regional impact risk; Species distribution modeling

1. Introduction

The introduction and spread of alien species pose significant threats to biodiversity, ecosystem functioning, and human livelihoods globally (Simberloff et al. 2013; Bellard et al. 2013; Roy et al. 2024). Non-native plants can alter habitat structure, disrupt nutrient cycling, reduce native species richness, and compromise agricultural productivity, generating both negative ecological and socio-economic impacts (Pyšek et al. 2012; Bacher et al. 2024). Accelerating globalization, anthropogenic activities, and climate change have increased both the rate and magnitude of alien species introductions, emphasizing the need for robust predictive tools to anticipate impacts and prioritize management interventions (Early et al. 2016). Accurate and spatially explicit assessments of potential impacts are critical for the efficient allocation of resources and the development of effective control strategies, particularly in countries with heterogeneous environmental conditions.

The Environmental Impact Classification for Alien Taxa (EICAT) provides a globally recognized framework for quantifying the environmental impacts of alien species (IUCN 2020). It classifies species along a gradient of impact severity, from minimal concern to massive impact, based on documented negative effects on native biodiversity (Blackburn et al. 2014; IUCN 2020). EICAT has been widely applied to advise prioritizing management interventions, inform conservation policies, and standardize assessments across taxa and regions (Kumschick et al. 2024). EICAT enables the assessment of local impact severity when reliable, region-specific data are available, but such documentation is often limited (Sohrabi et al. 2021). Consequently, the scarcity of local impact information constrains regional impact assessments, leading practitioners to rely on broader, global or multi-regional evaluations instead.

Species Distribution Models (SDMs) are powerful tools for predicting the potential distribution of species based on environmental variables such as climate, topography, land cover, and soil characteristics (Pradervand et al. 2014; Srivastava et al. 2019). By providing spatially explicit estimates of habitat suitability, SDMs offer valuable insights into where environmental conditions are favorable for the establishment and spread of alien species. This spatial information is particularly useful for complementing EICAT assessments when region-specific impact documentation is limited. By combining SDM-derived climate suitability with EICAT impact scores, regional impact assessments can more effectively link the severity of ecological impacts with the likelihood of

establishment. In this way, even species with moderate global- or national-level impact scores may pose high regional impacts where habitat conditions are favorable, whereas globally high-impact species may remain confined to unsuitable areas. This combined framework helps translate global impact assessments into regionally relevant evaluations and, when applied under future climate scenarios, allows identification of both current and emerging invasion hotspots, thereby supporting proactive, climate-adaptive management strategies.

For Iran, Sohrabi et al. (2021) evaluated 27 alien plant species using EICAT, largely relying on global impact scores due to the scarcity of local documentation. Their study identified several high-impact taxa, including *Pontederia crassipes* Mart. (water hyacinth), *Ailanthus altissima* (Mill.) (tree-of-heaven), *Imperata cylindrica* (L.) (cogon grass), *Ambrosia psilostachya* DC. (western ragweed), and *Paulownia fortunei* (Seem.) Hemsl (Chinese empress tree). From these, we selected 20 species with at least 30 occurrence records in Iran, minimizing extrapolation risks in subsequent SDMs. We first predicted species-specific climate suitability maps using SDMs, then combined these maps with EICAT impact scores. By integrating habitat suitability with impact severity, we derived a Regional Impact Risk Classification (RIRC) for each study species across Iran. We calculated RIRC under both current and future climate scenarios, producing species-specific RIRC maps as well as aggregated maps highlighting regions where high RIRC values from multiple species overlap. These overlay maps identify hotspots of potential invasion impact across Iran, providing a spatially explicit tool to guide regional management and prioritization of high-impact alien plants.

2. Methods

The RIRC framework was implemented in three main steps: (1) modeling the current and future climatic suitability for 20 alien plant species across Iran, (2) obtaining environmental impact classifications for these species using EICAT scores from Sohrabi et al. (2021), and (3) combining the suitability and impact data into a regional climate–impact risk matrix (Fig. 1).

2.1 Climatic suitability modelling for present and future conditions

Verified occurrence records for the 20 species (Table S1) were compiled from the Global Biodiversity Information Facility (GBIF.org 2024), the CABI Invasive Species Compendium, and Iranian literature databases (SID.ir; Magiran.com). To supplement global datasets, we systematically reviewed Iranian publications in both English and Persian to extract additional records. All occurrence records underwent quality checks: only georeferenced records with a spatial uncertainty of ≤100 m were retained, duplicates were removed, and spatial thinning was applied to maintain a maximum of one record per 1 km² grid cell, corresponding to the resolution of the environmental predictors.

Nineteen bioclimatic variables representing temperature and precipitation were obtained from the CHELSA v2.1 database (Karger et al. 2017), which provides climatic means from 1981 to 2010 at approximately 1 km resolution. To minimize multicollinearity, we calculated pairwise Spearman's rank correlations among predictors at occurrence locations. For highly correlated pairs ($|\rho| \geq 0.8$), we retained the ecologically more relevant variable. Variance Inflation Factor (VIF) analysis was also performed, excluding variables with a VIF of 10 or greater. The final set of predictors for each species is provided in Supplementary Material, Table S1.

Climatic suitability was modeled using Random Forests, implemented in the randomForest package (Liaw and Wiener 2002; randomForest v.4.7-1.1). Pseudo-absence points were generated through geographically stratified random sampling, with their number equal to that of the presence records for each species (Barbet-Massin et al. 2012).

Hyperparameters were optimized via 5-fold cross-validation, incorporating spatially structured folds to address potential spatial autocorrelation (Valavi et al. 2018). The Random Forest model was tuned by testing various values for two key parameters. For the first parameter, mtry, which specifies the number of predictor variables considered at each decision split, we tested values of 2, 3, 4, and 5. The second parameter, ntree, represents the number of decision trees grown in the forest; we evaluated 100, 200, 500, and 1000 trees. These ranges were selected based on preliminary trials and commonly used values in species distribution modeling. To ensure robust model evaluation, we applied repeated random subsampling validation, partitioning the dataset into 70% for training and 30% for testing over ten independent iterations (Teodorescu and Obreja Brașoveanu 2025). Model performance was assessed using out-of-bag (OOB) error for internal validation and external metrics (AUC and TSS)

for independent validation. Final models, parameterized with the optimal mtry and ntree values, were used to generate continuous climatic suitability maps for each species across Iran.

To assess climate change impacts, we used downscaled bioclimatic projections from CHELSA v2.1 (Karger et al. 2017) at ~1 km resolution, based on multiple global climate models (GCMs) under Representative Concentration Pathways (RCP) 4.5 (intermediate) and 8.5 (high) for the mid-century period (2041–2070). The ensemble suitability maps for each species were generated by combining predictions from SDM algorithms across five GCMs (GFDL-ESM4, UKESM1-0-LL, MPI-ESM1-2-HR, IPSL-CM6A-LR, and MRI-ESM2-0) into a single ensemble per scenario. Contributions from each algorithm were weighted according to the True Skill Statistic (TSS), following recommended practices in ecological forecasting (Samal, et al. 2022). This approach reduces algorithm-specific biases, captures inter-model climate variability, and produces robust projections of future species distributions.

2.2 Threshold selection

Continuous suitability values were converted into binary categories (suitable vs. unsuitable) using objective thresholding methods commonly applied in species distribution modeling (Jiménez-Valverde and Lobo 2007). Two criteria were compared: (i) Youden's J statistic (sensitivity + specificity – 1) and (ii) a prevalence-based threshold that aligned predicted prevalence with observed occurrence frequency. For each species, the more conservative threshold between these two was selected, thereby minimizing the risk of underestimating potential invasions for high-impact species with few occurrence records. Final thresholds are reported in the Supplementary Material (Table S1).

2.3 Combining climatic suitability and EICAT to produce RIRC

EICAT impact magnitudes for each species were obtained from Sohrabi et al. (2021) and categorized into five global impact levels: 1) Minimal Concern (MC): Indicating negligible effects on the native biota; 2) Minor (MN): Reduces individual performance in native biota without impacting population sizes; 3) Moderate (MO): Causes declines in the population size of at least one native taxon, but does not lead to local extinction; 4) Major (MJ): Induces community changes through local or sub-population extinction of at least one native taxon, with impacts that are naturally reversible if the alien

taxon is removed; 5) Massive (MV): Leads to naturally irreversible community changes through local, sub-population, or global extinction of at least one native taxon (IUCN 2020).

Climatic suitability values derived from SDMs were rescaled to a five-point ordinal scale (1 = unsuitable, 5 = optimal) using species-specific thresholds (see Table S1), ensuring that ecological thresholds accurately reflected individual habitat requirements. EICAT magnitudes were similarly converted to a 1–5 scale (MC = 1 … MV = 5) to align with SDM scores and give both indicators equal weight.

To integrate ecological impact and habitat suitability, local risk scores were calculated using a multiplicative approach (SDM × EICAT), resulting in an impact matrix with values ranging from 1 to 25. This method accounts for the joint influence of impact severity and establishment likelihood: areas with either low suitability or low impact are conservatively scored as lower risk. Multiplicative matrices have been widely applied in ecological risk assessments (Duijm 2015). The multiplicative model better differentiates higher RIRC scores compared to lower ones, aligning with our primary interest in prioritizing management attention for species predicted to have a higher impact.

Not all integer values between 1 and 25 are attainable when multiplying two 1–5 ordinal scales (e.g., 7, 13–14, and 17–19 are impossible), resulting in gaps in the range. Consequently, RIRC categories were defined based on the distribution of attainable scores and expert judgment to ensure ecologically meaningful classification. The resulting six-category RIRC is as follows (Fig. 1): Very Low (scores 1, 2, 3): Unsuitable or marginally suitable areas with MC, and unsuitable areas with MN. Low (scores 4, 5, 6)**:** Marginally suitable × MN, unsuitable × MO or MR, and moderately or highly suitable × MC. Moderate (scores 8, 9): Unsuitable × MV, marginally suitable × MO or MR, moderately suitable × MN or MO, highly suitable × MN, and optimal × MC. High (scores 10, 12): Marginally suitable × MV, moderately suitable × MR, highly suitable × MO, and optimal × MN. Very High (scores 15, 16): Moderately suitable × MV, highly suitable × MR, and optimal × MO. Extreme (scores 20, 25): Highly suitable × MV, and optimal areas × MR or MV.

To assess whether SDM predictive performance varied with ecological traits or impact level, species were grouped according to growth form (tree, shrub, vine, herb, grass, succulent, aquatic), photosynthetic pathway (C3, C4, CAM), habitat preference, and EICAT impact magnitude. Habitat

preference was determined from species occurrence points: each species was assigned to the habitat type in which it had the highest number of occurrences, with the top-ranked habitats being considered. EICAT impact magnitudes were categorized as low (Minimal [MC], Minor [MN]), moderate (Moderate [MO]), high (Major [MR] or Massive [MV]) concern. Differences in predictive metrics (accuracy, AUC, TSS) among categories within each group were evaluated using one-way ANOVA, with significance set at $p < 0.05$. Analyses were conducted in R version 4.4.1 (R Core Team 2024) using RStudio (Posit Team 2025).

3. Results

3.1 Model Performance

Model performance metrics for the 20 assessed alien plant species are summarized in Table S1. Test accuracies ranged from 90.3% for *Merremia dissecta* (Jacq.) Hallier f. (snake vine) to 99.2% for *Acacia saligna* (Labill.) H.L. Wendl (golden wreath wattle), with 12 species exceeding 95%. The corresponding AUC values varied between 0.928 and 0.992, with most species scoring above 0.96. True Skill Statistic (TSS) values ranged from 0.857 to 0.984. Precision, recall, and F1-scores were generally consistent across presence–absence classes, and out-of-bag (OOB) error rates were below 5% for most species. Predicted high-suitability areas varied among species, ranging from 18,432 km² for *P. fortunei* to 476,298 km² for *Cynanchum acutum* L. (stranglewort), reflecting differences in modeled habitat suitability.

No systematic differences were observed in predictive metrics relative to ecological traits (growth form: $p > 0.2$; photosynthetic pathway: $p > 0.32$; habitat preference: $p > 0.18$). Similarly, the species' EICAT impact magnitude did not affect model performance ($p > 0.34$).

3.2 Climatic Suitability Distributions

Climatic suitability maps reveal distinct spatial patterns, indicating that species have strong preferences for three main invasion hotspots (Fig. 2): the Caspian northern lowlands and Alborz foothills, the southern Persian Gulf and Gulf of Oman coast, and the Zagros foothills. In contrast, the central plateau and hyper-arid basins (Dasht-e Kavir and Dasht-e Lut) are unsuitable for most taxa.

To analyze these patterns, we formed functional groups consisting of species with similar life histories and ecological adaptations, assuming they have comparable habitat requirements and distributions.

Woody tree and shrub species. The present-day climatic suitability of *A. saligna* is concentrated along the southern and southwestern coasts and the Caspian shoreline, covering an area of 118,672 km² of high suitability. *Neltuma* (=*Prosopis) juliflora* SW. Raf. (mesquite) has the largest extent of high suitability among trees, dominating the southern coast and the southwestern Zagros foothills with 279,376 km². *Dalbergia sissoo* Roxb. Ex DC. (North Indian rosewood) also shows extensive high suitability across the southern and southwestern coastal lowlands and Zagros foothills, covering 112,430 km². *Ailanthus altissima* is primarily distributed in northern Iran, with high suitability in the Alborz foothills and adjacent provinces (49,071 km²). In contrast, *P. fortunei* exhibits fragmented high suitability in northern, northwestern, and localized southern areas, totaling 18,432 km², with low suitability across the interior plateau. High climatic suitability for *Bambusa vulgaris* Schrad. ex J.C. Wendl. (common bamboo) is indicated in narrow northern inland bands and fragmented southern coastal areas, covering 14,223 km².

Succulent and halophytic species. The suitability of succulents and coastal specialists is concentrated along southern coasts. *Opuntia ficus-indica* L. (Indian fig opuntia) shows high suitability in southern regions and selected inland pockets in the south-central area, covering 29,514 km². Meanwhile, the halophyte *Sesuvium portulacastrum* (L.) (shoreline purslane) creates a nearly continuous band of high suitability along the Persian Gulf and the Gulf of Oman coast, spanning 42,113 km².

Aquatic and semi-aquatic taxa. Across all three aquatic taxa, climate suitability is concentrated in the northern Caspian littoral wetlands, with additional but more fragmented suitable areas in the southwestern and southeastern lowlands. *Pistia stratiotes* L. (water Lettuce) shows the highest suitability along the Caspian coastal margin and across the western-southwestern lowland belt, covering approximately 33,212 km². *Pontederia crassipes* exhibits a similar but more spatially restricted pattern, with suitability largely confined to the Caspian plain (27,589 km²) and only minor isolated patches elsewhere. In contrast, *Azolla filiculoides* Lam. (water fern) displays the broadest distribution, with suitability extending beyond the Caspian region into the wetlands of Khuzestan and scattered depressions in southeastern Iran, totaling 12,549 km².

Herbaceous and vine species (fragmented patterns). *Ambrosia psilostachya* shows suitability areas in northern and western foothills (40,342 km²) with moderate suitability in Zagros and southern coastal patches. *Ammannia coccinea* Rottb. (valley redstem) suitabilities concentrates along southern and southeastern coasts (35,104 km²), while *Anoda cristata* (L.) (spurred anoda) and *M. dissecta* in southern and western parts of Iran (25,411 km² and 26,724 km², respectively). Suitable areas for *Euphorbia maculata* (L.) (spotted spurge) are inland northern hotspots (31,672 km²). *Cynanchum acutum* shows the broadest climatic range, with high suitability across Caspian lowlands, Alborz foothills, western Zagros, and southern coasts (476,298 km²).

Northern-focused herbaceous species. *Amsinckia menziesii* (Lehm.) (fiddleneck) is largely restricted to northern provinces, with high suitability in Caspian lowlands and Alborz foothills (21,684 km²) and moderate suitability extending into northwestern and western zones (9,874 km²), while central and southern regions remain mostly unsuitable. *Canna indica* L. (Indian shot) also shows high climatic suitability along the relatively wide Caspian Sea belt, with an additional patch of high suitability in the south and moderate suitability in parts of the Zagros foothills and the northwestern region of Iran.

Southern and southern-inland herbaceous species. *Imperata cylindrica* shows high suitability along the southern coast and in the provinces (29,874 km²), moderate suitability in the western lowlands and foothill margins, and low suitability in the northern highlands and central deserts.

Overall, the primary climatic hotspots for the studied alien species are the Caspian coast (north), the Persian Gulf–Oman coast (south), and the Zagros foothills (southwest). In contrast, the interior plateau and major desert basins are predicted to be unsuitable for most species under current climatic conditions.

Under mid-century climate projections (2041–2070) (Fig. 2), woody trees and shrubs generally show increased climatic suitability under both RCP 4.5 and RCP 8.5, except for *P. fortunei*, which expands moderately under RCP 4.5 but contracts substantially under RCP 8.5. Succulent and halophytic taxa (*O. ficus-indica*, *S. portulacastrum*) exhibit limited or no expansion under RCP 4.5 and display fragmented distributions under RCP 8.5. Aquatic and semi-aquatic species remain largely stable or show slight contraction under RCP 4.5 but expand markedly under RCP 8.5, particularly along

wetlands and hydrological corridors. Herbaceous species consistently expand their potential ranges, with the strongest gains projected under RCP 8.5 across the central, southern, and northern transitional zones. Detailed projections of these distributional shifts and their implications for RIRC are described in the following section.

3.3 Regional Impact Risk Classification (RIRC) Under Current and Future Climate Scenarios

The RIRC maps reveal significant spatial variations in the potential impact risk of 20 alien plants across Iran under current conditions and projected future climate scenarios (Fig. 3). Changes in spatial patterns and impact intensities reflect differences between the three scenarios. Under RCP 8.5, areas of higher potential impact are generally more extensive than under RCP 4.5, with expansions observed in northern humid regions, southern coastal zones, and parts of the central plateau.

Currently, extreme-impact RIRC zones are primarily concentrated along the northern Caspian Sea coast. Key species in these zones include *A. altissima*, *A. psilostachya*, *A. menziesii*, *A. filiculoides*, *P. fortunei*, *P. stratiotes*, and *P. crassipes*. The prevalence of these species in high-risk areas is primarily driven by their high climatic suitability rather than disproportionately high EICAT scores. Although several species (e.g., *A. altissima*, *A. psilostachya*, *P. crassipes*) are classified with major to massive global ecological impacts (EICAT = 4–5), their extensive suitable habitats in northern Iran (ranging from 12,500 to 49,000 km²) play a more significant role in elevating regional risk values. Under RCP 4.5, slight expansions and intensifications of these northern hotspots are projected, particularly for *A. altissima*, *A. psilostachya*, and *A. menziesii*. Under RCP 8.5, extreme-impact areas expand southward and inland, largely following increases in climatic suitability for aquatic and riparian taxa such as *A. filiculoides*, *P. stratiotes*, and *P. crassipes* (Fig. 2).

Extreme-impact zones are also identified in southern and southeastern regions under current conditions, particularly for *N. juliflora* (southeast, especially Sistan and Baluchestan), *D. sissoo* (southern coasts and southeast), *I. cylindrica* (southwestern coasts and Zagros Mountains), and *A. coccinea* (southern coasts). Under RCP 4.5, moderate intensifications are observed, including limited northward shifts of *N. juliflora*. Under RCP 8.5, expansions of *D. sissoo*, *I. cylindrica*, and *A. coccinea* are predicted in southwestern lowlands and higher elevations of the Zagros Mountains.

High-impact zones, often adjacent to extreme-impact areas, extend southward from the northern plateau into central regions and along southern coastal belts. Dominant species in these zones include *A. saligna* (southern and southwestern coasts), *E. maculata* (northern and central inland patches), and *M. dissecta* (southern and southwestern coasts). Under RCP 4.5, moderate expansions of *A. saligna* and *E. maculata* are expected. Under RCP 8.5, fragmented high-impact patches may appear in northwestern and northeastern provinces for *M. dissecta*.

Moderate-impact zones are associated with *A. saligna*, *A. coccinea*, *E. maculata*, *M. dissecta*, and *S. portulacastrum* (southern coastal fringes). No extreme-impact designations are present in this category under current conditions. RCP 4.5 results in minor changes, including slight reductions of *E. maculata* in northern patches. Under RCP 8.5, expansions of *S. portulacastrum* and *M. dissecta* into southwestern lowlands are observed.

Low- to very low-impact RIRC zones are recorded for *A. cristata* and *O. ficus-indica*, confined to small, fragmented southern coastal patches under current conditions. Under RCP 4.5, impact levels remain similar, while under RCP 8.5, slight increases are noted in coastal enclaves.

3.4 Cumulative RIRC Scores

Overlaying RIRC maps for all 20 species reveals cumulative regional impact patterns (Fig. 4). Under current conditions, the northern Caspian coastal plain displays the highest cumulative impact, characterized by overlapping extreme- and high-impact zones of *A. altissima*, *A. psilostachya*, *C. acutum*, *I. cylindrica*, *A. filiculoides*, *P. fortunei*, *P. stratiotes*, and *P. crassipes*. Moderate to high cumulative overlap is observed along southwestern coastal areas near the Persian Gulf, primarily involving *A. filiculoides*, *M. dissecta*, *A. saligna*, and *D. sissoo*.

Under RCP 4.5, slight intensification of impacts and expansion of suitable areas are predicted in the northern Caspian region for *A. altissima* and *C. acutum*. Southwestern coastal areas show moderate broadening of cumulative impact risk for *A. saligna* and *D. sissoo*. Under RCP 8.5, these expansions become more extensive, with the northern Caspian region exhibiting southward incursions into the northern plateau, where *P. stratiotes* and *I. cylindrica* form larger clusters. Southwestern coastal zones also experience further inland penetration by *M. dissecta* and *A. filiculoides*.

Eastern deserts, the central plateau, and arid regions (Dasht-e Kavir and Dasht-e Lut) exhibit minimal cumulative impacts under current conditions. Under RCP 4.5, only marginal increases are observed for *N. juliflora* and *S. portulacastrum*. Under RCP 8.5, slight intensifications are detected, with *O. ficus-indica* and *A. cristata* showing minor high-impact patches.

The northwestern mountainous region contains limited moderate-impact zones under current conditions, involving *A. cristata* and *E. maculata*. Under RCP 4.5, small expansions occur for *E. maculata*. Under RCP 8.5, increases are noted for *E. maculata* and *A. coccinea* at higher elevations. The southeastern periphery, dominated by *N. juliflora* and *A. coccinea*, shows negligible cumulative impact under current conditions and limited increases under RCP 4.5. Slight increases are observed under RCP 8.5.

Net changes in the number of species contributing to increased or decreased RIRC values per pixel across Iran under the two future climate scenarios are presented in Fig. 5. Under RCP 4.5, northern Caspian coastal regions show increases in RIRC-contributing species ranging from 4 to 6 species, while the southern Persian Gulf lowlands show increases of 1 to 3 species. In contrast, decreases involving 1 to 3 species are observed across the central plateau and arid interior regions. Under RCP 8.5, the number of species associated with increased RIRC values rises to 7 to 9 in the northern coasts and 4 to 6 in the southern lowlands, while 4 to 6 species show decreased contributions in the central deserts. Eastern deserts, the central plateau, and other arid zones exhibit minimal net changes (0 to ±3 species). Northwestern mountainous areas indicate increases of 1 to 3 species under RCP 4.5, rising to 4 to 6 species under RCP 8.5, primarily driven by *E. maculata* and *A. coccinea*. Southeastern peripheral areas remain largely stable, with *O. ficus-indica* showing no change.

Projected mean changes in RIRC vary among species and climate scenarios (Fig. 6). Under both RCP 4.5 and RCP 8.5, species such as *A. saligna*, *C. acutum*, *M. dissecta*, and *O. ficus-indica* are predicted to significantly increase their RIRC contributions, with more pronounced gains expected under RCP 8.5. *N. juliflora* shows stronger increases under RCP 4.5. In contrast, several woody and aquatic species, including *P. fortunei* (RCP 8.5), *P. stratiotes* and *P. crassipes* (RCP 4.5), and *S. portulacastrum* (both scenarios), are projected to reduce their contributions to RIRC, with the greatest decreases occurring under the more extreme RCP 8.5 scenario.

4. Discussion

Our integrated approach, combining EICAT with SDMs, provides a framework for examining where alien plants may establish and exert ecological impacts. By intersecting species-specific impact magnitudes with climatic suitability, the RIRC framework produces maps that highlight areas where potential impacts may coincide with favorable environmental conditions. These outputs offer regionally relevant information for decision-making while remaining consistent with currently available evidence.

Most EICAT scores for the 20 species assessed in this study were sourced from global evaluations (Sohrabi et al. 2021) due to the scarcity of local impact data in Iran, but they provide a consistent basis for a comparative assessment. In this context, RIRC adds an evidence-based spatial layer to existing impact magnitudes, offering a structured approximation of potential regional risk where local studies are lacking. Although not a substitute for field-derived impact assessments, this combined approach can be useful in data-poor systems and guide future research priorities.

Because RIRC is environmentally driven, projections under future climate scenarios translate into potential shifts in impact risk distribution. For example, drought- and salt-tolerant species such as *N. juliflora* may find more favorable conditions in parts of the semi-arid interior under warming scenarios (Shiferaw et al. 2004; Richardson and Rejmánek 2011). Coupling SDMs with EICAT facilitates spatial visualization of potential future invasion impacts and supports forward-looking management strategies. Risk maps and impact matrices derived from this integration serve as decision-support tools, translating complex ecological assessments into formats relevant for environmental planning (Gallien et al. 2012; Guisan et al. 2013).

This combined framework can also assist in prioritizing taxa that show high climatic suitability and high ecological impact potential. For instance, *Ailanthus altissima*, a disturbance-adapted tree with documented effects across various ecosystems (Kowarik and Säumel 2007; Sladonja et al. 2015), illustrates how spatial suitability and impact magnitude can align in several parts of Iran. Invasion dynamics across Iran are shaped by the country's climatic and ecological heterogeneity. These patterns correspond with areas of moderate climatic stress, higher water availability, and disturbance levels that facilitate the establishment and spread of invasive species. These outcomes align with

broader ecological principles: invasion success tends to decline where climatic stress exceeds species' tolerance thresholds, while mesic microclimates and human-modified environments provide ecological opportunities (Bisht et al. 2024; Oveisi et al. 2025). Even drought-adapted taxa typically depend on episodic water inputs from precipitation, irrigation, or runoff, highlighting the importance of hydrological dynamics in shaping invasion pathways in dryland systems (Van Loon et al. 2024).

Life-form differences create distinct spatial patterns in potential impact. Woody perennials benefit from riparian corridors and foothill mosaics where groundwater availability and moderated temperatures support persistence (Atasoy et al. 2018). Aquatic macrophytes are associated with nutrient-enriched and hydrologically stable habitats, while herbaceous ruderals and climbing vines follow transport networks, agricultural landscapes, and other disturbed margins (Thomaz et al. 2025). These patterns reflect interactions between life-history strategies and local environmental constraints.

Of Iran's invasion hotspots, the northern Caspian coastal plain is the one needing the most urgent attention, where extreme- and high-impact zones support *A. altissima*, *A. psilostachya*, *C. acutum*, *A. menziesii*, and aquatic invaders such as *A. filiculoides*, *P. stratiotes*, and *P. crassipes*. Species with exceptionally broad high-impact zones, like *C. acutum*, are projected to become even more problematic under future climate scenarios. The southern and southeastern regions, including Sistan–Baluchestan, the Gulf of Oman coast, and the Zagros foothills, represent the second most critical priority area, driven by *N. juliflora*, *D. sissoo*, *I. cylindrica*, and *A. coccinea*.

Under future scenarios (RCP 4.5 and 8.5), the northern Caspian is expected to become increasingly vulnerable, particularly to the expansion of aquatic and riparian species. In contrast, southern and southwestern coastal–foothill ecotones are likely to show greater suitability for woody and herbaceous invaders. Additionally, the northwestern highlands are emerging as new high-risk zones for *E. maculata* and *A. coccinea*.

These findings highlight the urgent need for region-specific strategies that emphasize early detection and rapid response to prevent establishment. Monitoring efforts should be prioritized for hydrological corridors in the north, plantations and ports in the south, and sentinel plots at high-elevation boundaries**.** At the national level, implementing predictive pathway management, climate-informed reprioritization of hotspots, and strategically deployed detection teams is essential. The RIRC

framework supports these initiatives by providing a structured, spatially resolved approach to identify priority areas, anticipate invasion risks under current and future climates, and guide targeted monitoring and rapid intervention.

Future developments of the RIRC framework could integrate land-use and land-cover patterns, soil characteristics, hydrological variables, and indicators of anthropogenic strain. This would enable a more comprehensive understanding of the factors influencing establishment likelihood and impact magnitude, especially in rapidly changing environments. Expanding local impact studies will further refine EICAT scores and reduce reliance on global assessments. Finally, measuring impact magnitudes locally and comparing them to the model estimates is needed to validate and further improve our approach.

Overall, RIRC offers a structured and spatially resolved approach for examining potential invasion impacts under current and future climates. Despite data limitations and modeling uncertainties, it is intended as a quantitative tool for identifying areas where focused monitoring, field assessment, or management attention may be most timely and beneficial.

5. **Conclusion**

Acknowledgement

MO acknowledges support from the Swiss National Science Foundation (Scientific Exchange grant IZSEZ0_204050). YS acknowledges funding from the National Natural Science Foundation of China (grant 32522062) and the Fundamental Research Funds for the Central Universities (grant 2662025ZHPY003). SB acknowledges support from the Swiss National Science Foundation (grant IC00I0-231475). HMS acknowledges funding from the Swiss National Science Foundation (grant 31003A_166448).

References

Atasoy M, Anderson CJ, Guneysu Atasoy F (2018) Evaluating the distribution of invasive woody vegetation around riparian corridors in relation to land use. Urban Ecosystems 21(2): 459-466. https://doi.org/10.1007/s11252-017-0729-3.

Bacher S, Galil BS, Nuñez MA, Ansong M, Cassey P, Dehnen-Schmutz, K, Fayvush G, Hiremath AJ, Ikegami M, Martinou AF, McDermott SM, Preda C, Vilà M, Weyl OLF, Fernandez RD, Ryan-Colton E (2024) IPBES Invasive Alien Species Assessment: Chapter 4. Impacts of invasive alien species on nature, nature's contributions to people, and good quality of life (Version 4) Zenodo. https://doi.org/10.5281/zenodo.10677193.

Bellard C, Jeschke JM, Leroy B, Mace GM (2018) Insights from modeling studies on how climate change affects invasive alien species geography. Ecology and Evolution 00: 1-13. https://doi.org/10.1002/ece3.4098.

Bellard C, Thuiller W, Leroy B, Genovesi P, Bakkenes M, Courchamp F (2013) Will climate change promote future invasions?. Global Change Biology 19(12): 3740–3748. https://doi.org/10.1111/gcb.12344.

Bisht S, Rawat GS, Bargali SS, Rawat YS, Mehta A (2024) Forest vegetation response to anthropogenic pressures: a case study from Askot Wildlife Sanctuary, Western Himalaya. Environment, Development and Sustainability 26(4): 10003-10027. https://doi.org/10.1007/s10668-023-03130-2.

Blackburn TM, Essl F, Evans T, Hulme PE, Jeschke JM, Kühn I, Kumschick S, Marková Z, Mrugała A, Nentwig W, Pergl J, Pyšek P, Rabitsch W, Ricciardi A, Richardson DM, Sendek A, Vilà M, Wilson JR, Winter M, Genovesi P, Bacher S. (2014) A unified classification of alien species based on the magnitude of their environmental impacts. PLoS biology 12(5): p.e1001850. https://doi.org/10.1371/journal. pbio. 1001850.

Duijm NJ (2015) Recommendations on the use and design of risk matrices. Safety science 76:21-31. https://doi.org/10.1016/j.ssci.2015.02.014.

Early R, Bradley BA, Dukes JS, Lawler JJ, Olden JD, Blumenthal DM, Gonzalez P, Grosholz ED, Ines I, Miller LP, Sorte CJB, Tatem AJ (2016) Global threats from invasive alien species in the twenty-first century and national response capacities Nature Communications 7: 12485. https://doi.org/10.1038/ncomms12485.

Gallien L, Douzet R, Pratte S, Zimmermann NE, Thuiller W (2012) Invasive species distribution models—How violating the equilibrium assumption can create new insights. Global Ecology and Biogeography 21(11): 1126–1136. https://doi.org/10.1111/j.1466-8238.2012.00768.x.

GBIF Secretariat. 2024. GBIF.org [Database]. Global Biodiversity Information Facility. https://www.gbif.org

Guisan A, Tingley R, Baumgartner JB, Naujokaitis-Lewis I, Sutcliffe PR, Tulloch AIT, Regan TJ. Brotons L, McDonald-Madden E, Mantyka-Pringle C, Martin TG, Rhodes JR, Maggini R, Setterfield SA, Elith J, Schwartz MW, Wintle BA, Broennimann O, Austin M, Ferrier S, Kearney MR, Possingham HP, Buckley YM (2013) Predicting species distributions for conservation decisions. Ecology Letters 16(12): 1424–1435. https://doi.org/10.1111/ele.12189.

IUCN. 2020. IUCN EICAT Categories and Criteria. The Environmental Impact Classification for Alien Taxa First edition. Gland, Switzerland and Cambridge, UK. https://doi.org/10.2305/IUCN.CH.2020.05.en.

Jiménez-Valverde A, Lobo JM (2007) Threshold criteria for conversion of probability of species presence to either-or presence–absence. Acta Oecologica 31(3): 361–369. https://doi.org/10.1016/j.actao.2007.02.001.

Karger DN, Conrad O, Böhner J, Kawohl T, Kreft H, Soria-Auza RW, Zimmermann NE, Linder HP, Kessler M (2017) Climatologies at high resolution for the earth's land surface areas. Scientific Data 4(170122): 1–20. https://doi.org/10.1038/sdata.2017.122.

Kowarik I, Säumel I (2007) Biological flora of Central Europe: *Ailanthus altissima* (Mill.) Swingle. Perspectives in Plant Ecology, Evolution and Systematics 8(4): 207–237. https://doi.org/10.1016/j.ppees.2007.03.002.

Kumschick S, Bertolino S, Blackburn TM, Brundu G, Costello KE, De Groot M, Evans T, Gallardo B, Genovesi P, Govender T, Jeschke JM, Lapin K, Measey J, Novoa A, Nunes AL, Probert AF, Pyšek P, Preda C, Rabitsch W, Roy HE, Smith KG, Tricarico E, Vilà M, Vimercati G, Bacher S (2024) Using the IUCN Environmental Impact Classification for Alien Taxa to inform decision-making. Conservation Biology 38(2): e14214. https://doi.org/10.1111/cobi.14214

Liaw A, Wiener M (2002) Classification and Regression by Randomforest. R News 2: 18-22. http://CRAN.R-project.org/doc/Rnews/

Magiran (2024) Magiran.com [Database]. https://www.magiran.com

Oveisi M, Sohrabi S, Piri R, Mueller Schaere H (2025) Observed Distribution and predicted further Spread of *Araujia sericifera* from Europe to the Southern Caspian Sea Coast. Weed Research 0:1–12, https://doi.org/10.1111/wre.70041

Pradervand JN, Dubuis A, Pellissier L, Guisan A, Randin C (2014) Very high resolution environmental predictors in species distribution models: Moving beyond topography? Progress in Physical Geography: Earth and Environment 38(1): 79–96. https://doi.org/10.1177/0309133313512667.

Pyšek P, Jarošík V, Hulme PE, Pergl J, Hejda M, Schaffner U, Vilà M (2012) A global assessment of invasive plant impacts on resident species, communities and ecosystems: the interaction of impact measures, invading species' traits and environment. Global Change Biology 18(5): 1725–1737. https://doi.org/10.1111/j.1365-2486.2011.02636.x.

Richardson DM, Rejmánek M (2011) Trees and shrubs as invasive alien species – A global review. Diversity and Distributions 17(5): 788–809. https://doi.org/10.1111/j.1472-4642.2011.00782.x.

Roy HE, Pauchard A, Stoett P, Renard Truong T, Bacher S, Galil BS, Hulme PE, Ikeda T, Sankaran K, McGeoch MA, Meyerson LA, Nuñez MA, Ordonez A, Rahlao SJ, Schwindt E, Seebens H,

Shepparrd AW, Vandvik V (2024) IPBES Invasive Alien Species Assessment: Summary for Policymakers (Version 3). Zenodo. https://doi.org/10.5281/zenodo.11254974.

R Core Team (2024) R: A Language and Environment for Statistical Computing. R Foundation for Statistical Computing, Vienna, Austria. URL: https://www.R-project.org/

Posit team (2025) RStudio: Integrated Development Environment for R. Posit Software, PBC, Boston, MA. URL: http://www.posit.co/

Samal P, Srivastava J, Singarasubramanian SR, Saraf PN, Charles B (2022) Ensemble modeling approach to predict the past and future climate suitability for two mangrove species along the coastal wetlands of peninsular India. Ecological Informatics 72: 101819. https://doi.org/10.1016/j.ecoinf.2022.101819.

Shiferaw H, Teketay D, Nemomissa S, Assefa F (2004) Some biological characteristics that foster the invasion of *Prosopis juliflora* (Sw.) DC. at Middle Awash Rift Valley Area, northeastern Ethiopia. Journal of Arid Environments 58(2): 135–154. https://doi.org/10.1016/j.jaridenv.2003.08.011.

SID (2024) SID.ir [Database] Scientific Information Database. https://www.sid.ir

Simberloff D, Martin JL, Genovesi P, Maris V, Wardle DA, Aronson J, Courchamp F, Galil B, García-Berthou E, Pascal M, Pyšek P, Sousa R, Tabacchi E, Vilà (2013) Impacts of biological invasions: What's what and the way forward. Trends in Ecology & Evolution 28(1), 58–66. https://doi.org/10.1016/j.tree.2012.07.013.

Sladonja B, Sušek M, Guillermic J (2015) Review on invasive tree of heaven (*Ailanthus altissima* (Mill.) Swingle): Spread, ecological impacts, and control management. Environmental Management 56: 1009–1034. https://doi.org/10.1007/s00267-015-0546-5.

Sohrabi S, Pergl J, Pyšek P, Foxcroft LC, Gherekhloo J (2021) Quantifying the potential impact of alien plants of Iran using the Generic Impact Scoring System (GISS) and Environmental Impact Classification for Alien Taxa (EICAT). Biological Invasions 23(8): 2435–2449. https://doi.org/10.1007/s10530-021-02515-6.

Srivastava V, Lafond V, Griess VC (2019) Species distribution models (SDM): Applications, benefits and challenges in invasive species management. CAB Reviews 14(020): 1–13. https://doi.org/10.1079/PAVSNNR201914020

Teodorescu V, Obreja Brașoveanu L (2025) Assessing the validity of k-fold cross-validation for model selection: Evidence from bankruptcy prediction using random forest and XGBoost. Computation 13(5): 127. https://doi.org/10.3390/computation13050127.

Thomaz SM, Cardozo ALP, Quirino BA, Yofukuji KY, Aleixo MHF, Fugi R (2025) A review of the ecological role of aquatic macrophytes on freshwater fish. Hydrobiologia 852(13):3257-3290. https://doi.org /10.1007/s10750-025-05819-z

Valavi R, Elith J, Lahoz-Monfort JJ, Guillera-Arroita G (2018) *blockCV*: An R package for generating spatially or environmentally separated folds for k-fold cross-validation of species distribution models. bioRxiv 357798. https://doi.org/10.1111/2041-210X.13107

Van Loon AF, Kchouk S, Matanó A, Tootoonchi F, Alvarez-Garreton C, Hassaballah KEA, Wu M, Wens MLK, Shyrokaya A, Ridolfi E, Biella R, Nagavciuc V, Barendrecht MH, Bastos A, Cavalcante L, de Vries FT, Garcia M, Mård J, Streefkerk IN, Teutschbein C, Tootoonchi R, Weesie R, Aich V, Boisier JP, Di Baldassarre G, Du Y, Galleguillos M, Garreaud R, Ionita M, Khatami S, Koehler JKL, Luce CH, Maskey S, Mendoza HD, Mwangi MN, Pechlivanidis IG, Ribeiro Neto GG, Roy T, Stefanski R, Trambauer P, Koebele EA, Vico G, Werner M (2024) Review article: Drought as a continuum–memory effects in interlinked hydrological, ecological and social systems. Natural Hazards and Earth System Sciences 24(9): 3173-3205. https://doi.org/10.5194/nhess-24-3173-2024.

Table S1. Model performance (Correlation, TSS, AUC), EICAT magnitude, ecological traits (habitat, life history, growth form), introduction pathway and origin, major impact mechanisms, variables retained after multicollinearity test, and estimated high-suitability area (km²) for the 20 alien plant species studied.

Species	Corr.	TSS	AUC	EICAT	Habitat	Life history	Growth form	Pathway	Origin (source)	Major impact mechanisms	Variables kept after VIF	High-suitability area (km²)
Acacia saligna	0.9847	0.9847	0.992	3	Disturbed sand dunes, riparian, coastal areas	Perennial	Shrub/tree	C3	Australia (CABI)	Structural impact on ecosystem	bio1, bio14, bio15, bio18, bio19, bio3, bio4, bio8, bio9	118,672
Ailanthus altissima	0.9696	0.9697	0.985	4	Urban areas, roadsides, waste ground	Perennial	Tree	C3	China/Taiwan (CABI)	Competition, toxicity, structural & chemical impacts	bio10, bio13, bio14, bio15, bio19, bio3, bio6, bio8, bio9	49,071
Ambrosia psilostachya	0.9616	0.9617	0.981	4	Grasslands, roadsides	Perennial	Herb	C3	North America (CABI)	Competition, toxicity, hybridisation, herbivory	bio1, bio13, bio15, bio18, bio19, bio2, bio4, bio8, bio9	40,342
Ammannia coccinea	0.9377	0.9380	0.969	2	Wetlands, disturbed sites	Annual / Perennial	Herb	C3	North America (Jepson, CABI)	Competition, toxicity, hybridization	bio10, bio13, bio14, bio15, bio18, bio19, bio2, bio3, bio8, bio9	35,104
Amsinckia menziesii	0.932	0.940	0.972	-	Grasslands, disturbed sites, roadsides, fields	Annual	Herb	C3	Western North America (native, weed outside)	Toxicity (livestock poisoning), competition	bio1, bio13, bio15, bio18, bio19, bio2, bio4, bio8, bio9	20140
Anoda cristata	0.9383	0.9386	0.969	3	Disturbed sites, waste ground	Annual	Herb	C3	Americas (CABI, floras)	Competition, disease transmission	bio1, bio15, bio18, bio19, bio3, bio4, bio8	25,411
Azolla filiculoides	0.9518	0.9519	0.976	3	Aquatic, wetlands	Perennial	Aquatic fern	C3	Americas (CABI)	Competition, biofouling, structural impacts	bio13, bio14, bio15, bio18, bio19, bio2, bio3, bio8, bio9	12,549

Bambusa vulgaris	0.8857	0.8862	0.943	3	River banks, open ground	Perennial	Bamboo	C3	Tropical Asia (CABI)	Competition	bio1, bio13, bio14, bio15, bio18, bio19, bio2, bio3, bio4, bio8, bio9	14,223
Canna indica	0.9213	0.9420	0.969	3	Wetland edges, swamp margins, streambanks, moist disturbed sites, gardens	Perennial	Herb / rhizomatous herb	C3	Tropical America (native)	Competition, displacement via rhizomes	bio13, bio14, bio15, bio18, bio19, bio2, bio3, bio8, bio9	13350
Cynanchum acutum	0.9667	0.9668	0.983	3	Wetlands, disturbed areas	Perennial	Vine	C3	Mediterranean / Asia (CABI)	—	bio13, bio14, bio15, bio18, bio19, bio2, bio3, bio4, bio8, bio9	476,298
Dalbergia sissoo	0.8860	0.8867	0.943	2	River banks, alluvial soils	Perennial	Tree	C3	Indian subcontinent (CABI)	—	bio13, bio14, bio15, bio18, bio19, bio2, bio3, bio4, bio8, bio9	112,430
Euphorbia maculata	0.9525	0.9527	0.976	2	Disturbed areas, lawns	Annual	Herb	C4	North America (CABI)	Competition	bio10, bio12, bio14, bio15, bio18, bio2, bio4, bio8, bio9	31,672
Imperata cylindrica	0.9623	0.9623	0.981	4	Grasslands, plantations	Perennial	Grass	C4	SE Asia / E Africa (CABI)	—	bio10, bio13, bio14, bio15, bio18, bio19, bio2, bio3, bio8, bio9	29,874
Merremia dissecta	0.8576	0.8592	0.928	2	Disturbed sites, thickets	Perennial	Vine	C3	Tropical Americas (CABI)	—	bio13, bio14, bio15, bio18, bio19, bio2, bio3, bio4, bio8, bio9	26,724
Neituma(=Prosopis) juliflora	0.9078	0.9087	0.953	3	Arid rangelands, saline soils	Perennial	Tree/shrub	C3	Mexico / South America (CABI)	Structural & chemical impacts	bio10, bio13, bio14, bio15, bio18, bio19, bio2, bio3, bio8, bio9	279,376

Opuntia ficus-indica	0.9603	0.9603	0.980	2	Arid / semi-arid, disturbed	Perennial	Cactus / shrub	CAM	Mexico (CABI)	Competition, toxicity, chemical impacts	bio10, bio11, bio13, bio14, bio15, bio18, bio19, bio2, bio3, bio8, bio9	29,514
Paulownia fortunei	0.9082	0.9083	0.954	3	Riversides, forests	Perennial	Tree	C3	SE China (CABI)	Chemical ecosystem impacts	bio10, bio11, bio13, bio14, bio15, bio18, bio19, bio2, bio8, bio9	18,432
Pistia stratiotes	0.8884	0.8892	0.944	3	Aquatic ponds, rivers	Perennial	Floating herb	C3	Africa / S. America (CABI)	Structural impacts	bio15, bio18, bio19, bio2, bio3, bio8, bio9	33,212
Pontederia crassipes	0.9103	0.9109	0.955	4	Aquatic rivers, lakes	Perennial	Aquatic herb	C3	South America (CABI)	Structural, competition, biofouling	bio10, bio13, bio14, bio15, bio18, bio19, bio2, bio3, bio8, bio9	27,589
Sesuvium portulacastrum	0.9329	0.9330	0.966	1	Coastal saline areas	Perennial	Succulent herb	C4	Tropics / subtropics (CABI)	Competition, toxicity	bio10, bio13, bio14, bio15, bio18, bio19, bio2, bio3, bio8, bio9	42,113

562

563

564

565

566

567

568

569

Figure Captions

Figure 1. Schematic workflow for the development of the Regional Impact Risk Classification (RIRC). EICAT assessment scores were obtained from Sohrabi et al. (2021).

Figure 2. Climate suitability maps for 20 alien plant species of Iran under current and future climate scenarios (RCP 4.5 and RCP 8.5; 2041–2070).

Figure 3. Regional Impact Risk Classification (RIRC) maps for 20 alien plant species of Iran, showing the spatial distribution of impact risk categories under current and future climate scenarios (RCP 4.5 and RCP 8.5; 2041–2070).

Figure 4. Cumulative RIRC impact map, generated by overlaying the individual RIRC maps of 20 alien species, highlighting regional hotspots with highest levels of potential ecological impact.

Figure 5. Overlay maps showing the number of species with increasing or decreasing RIRC scores at each location under two future climate change scenarios, highlighting spatial patterns of cumulative future invasion risk across the study area

Figure 6. Mean change in RIRC for the 20 alien plant species under two climate change scenarios (RCP 4.5 and RCP 8.5).

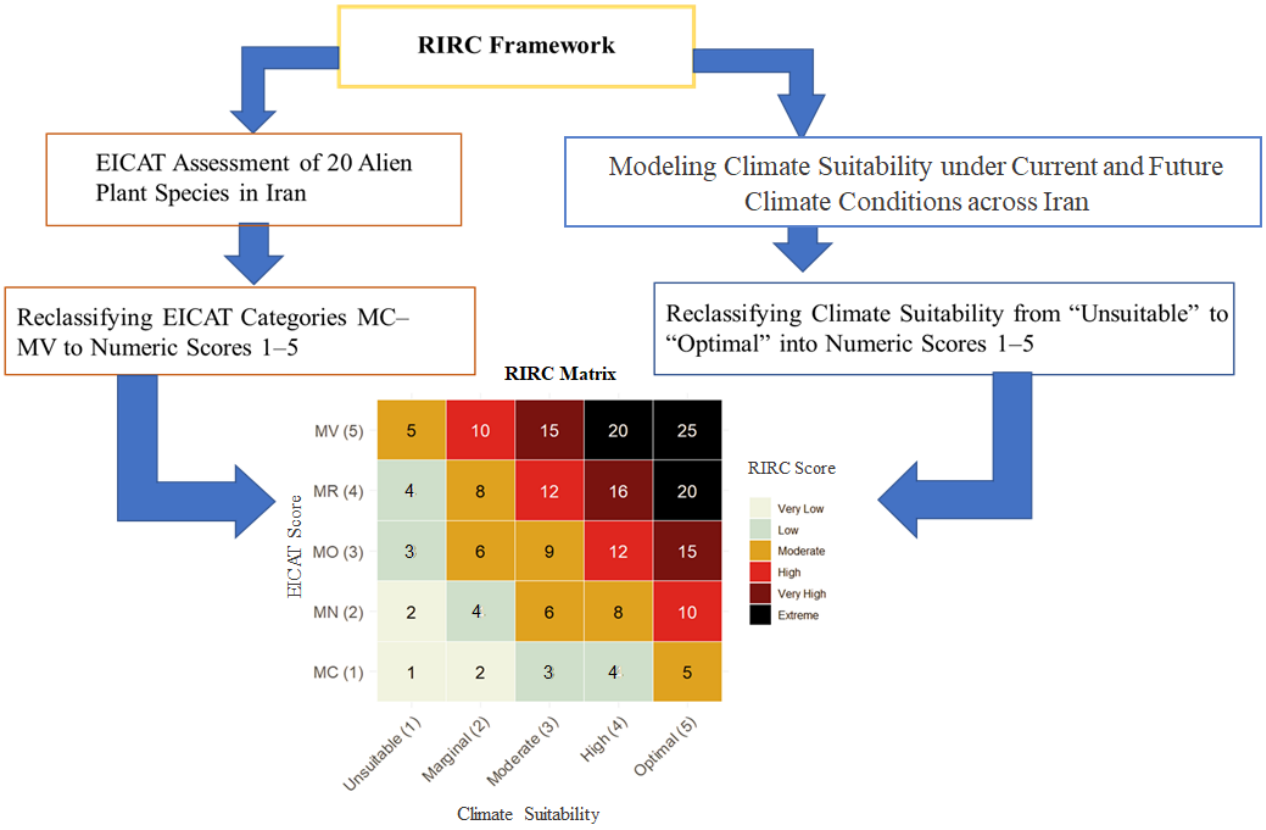
RIRC Framework
EICAT Assessment of 20 Alien Plant Species in Iran
Modeling Climate Suitability under Current and Future Climate Conditions across Iran
Reclassifying EICAT Categories MC–MV to Numeric Scores 1–5
Reclassifying Climate Suitability from "Unsuitable" to "Optimal" into Numeric Scores 1–5
RIRC Matrix
EICAT Score
MV (5) 5 10 15 20 25
MR (4) 4 8 12 16 20
MO (3) 3 6 9 12 15
MN (2) 2 4 6 8 10
MC (1) 1 2 3 4 5
Unsuitable (1)
Marginal (2)
Moderate (3)
High (4)
Optimal (5)
Climate Suitability
RIRC Score
Very Low
Low
Moderate
High
Very High
Extreme

Figure 1.

605

Woody tree and shrub species:

Acacia saligna

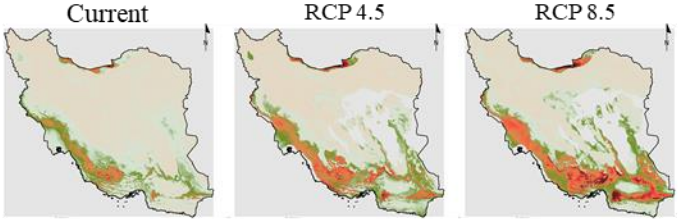

Ailanthus altissima

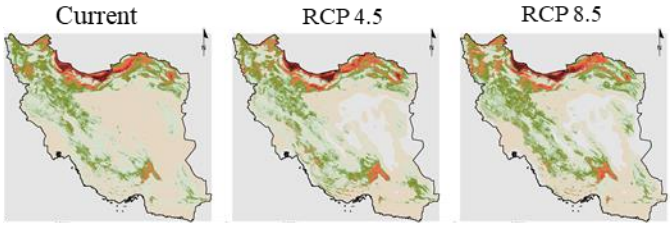

Dalbergia sissoo

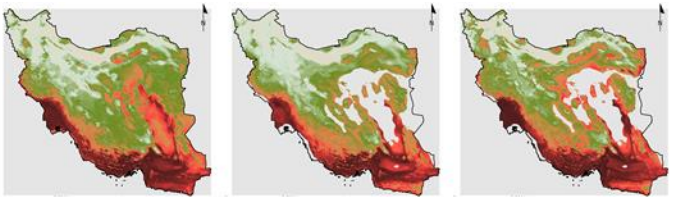

Neltuma juliflora

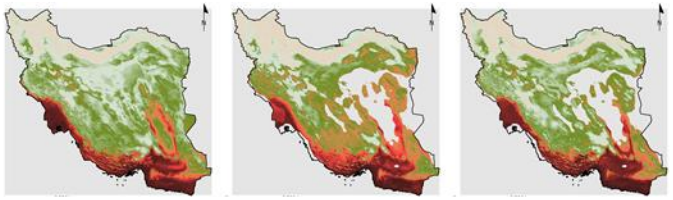

Bambusa vulgaris

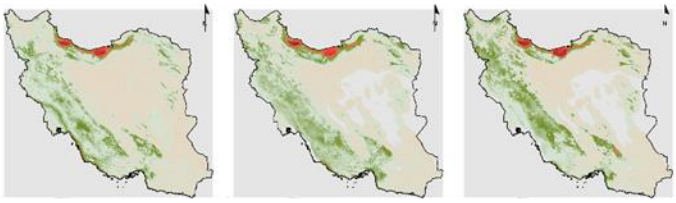

Paulownia fortunei

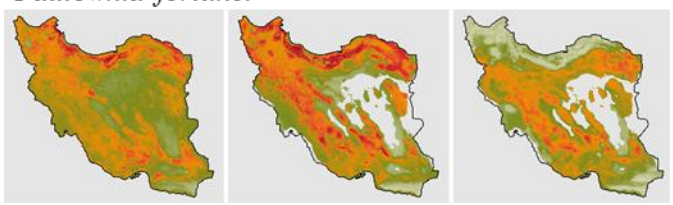

Succulent and halophytic species:

Opuntia ficus-indica

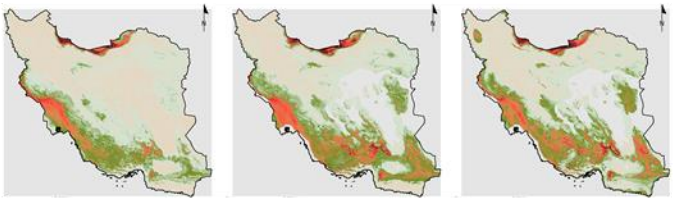

Sesuvium portulacastrum

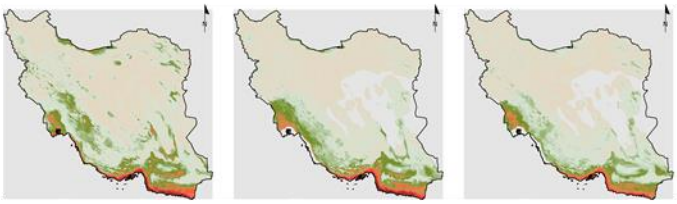

Aquatic and semi-aquatic taxa:

Pistia stratiotes

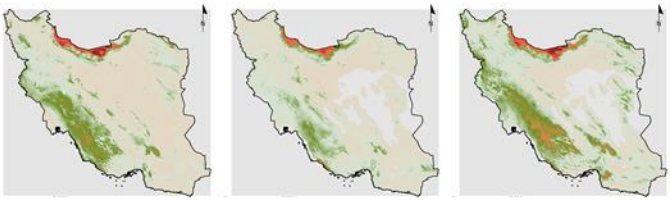

Pontederia crassipes

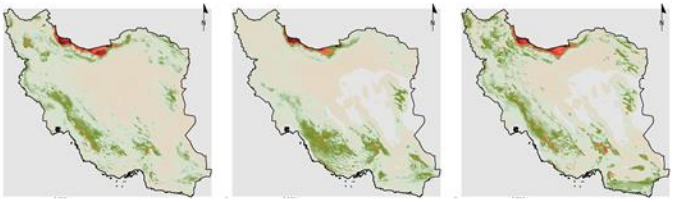

Azolla filiculoides

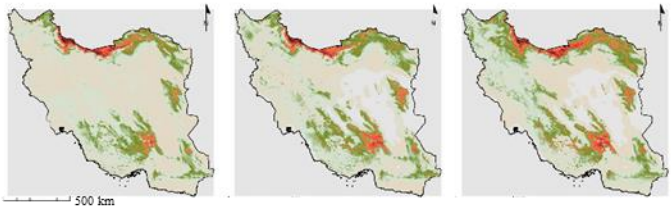

606

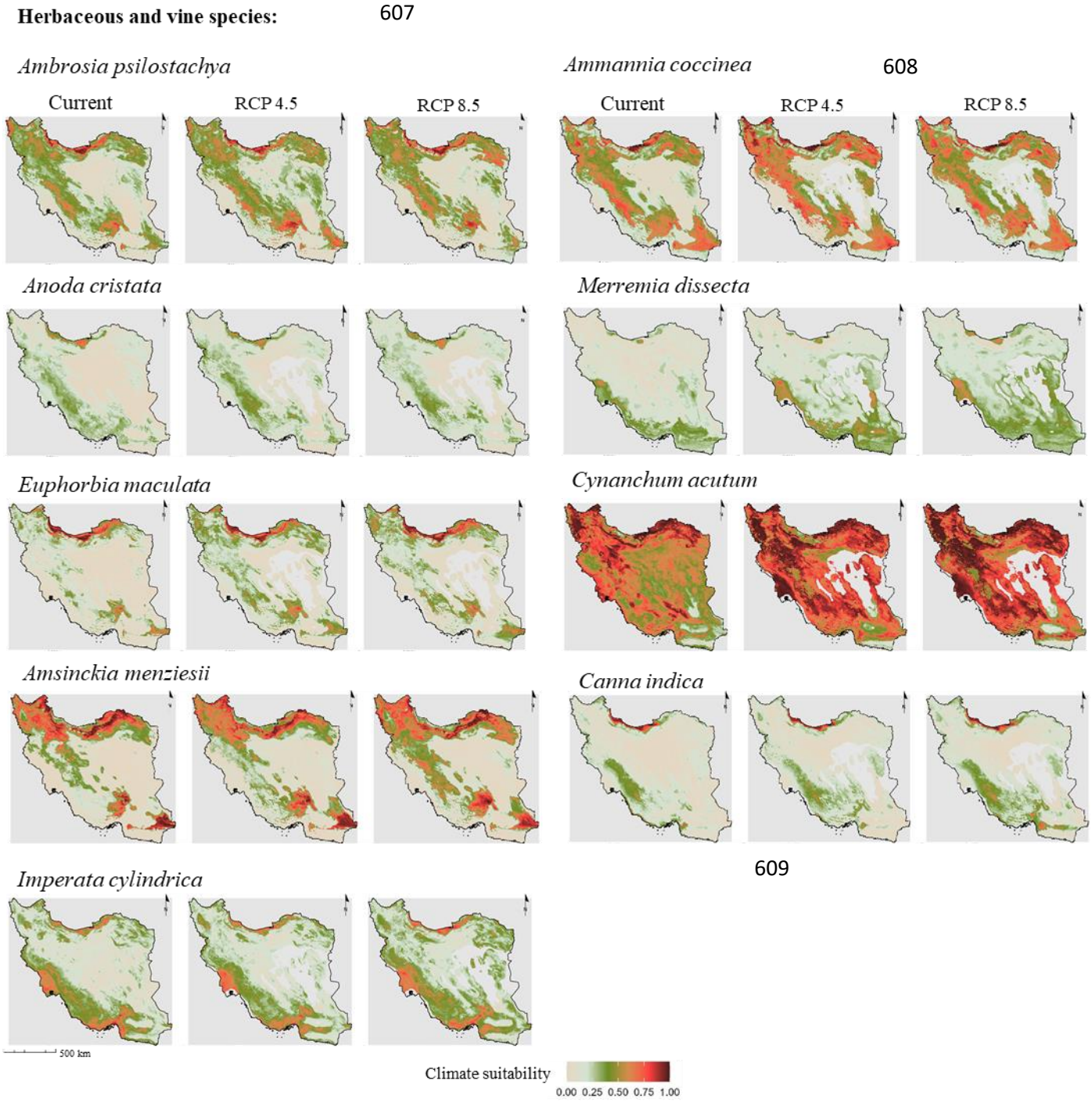

613

614 **Figure 2.**

615

616

617

Woody tree and shrub species:

Acacia saligna

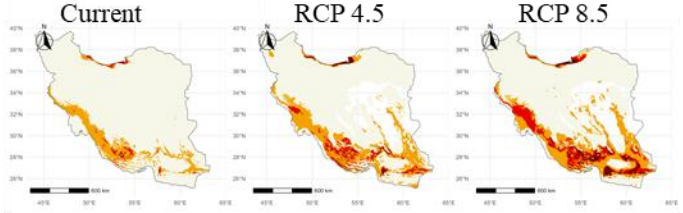

Ailanthus altissima

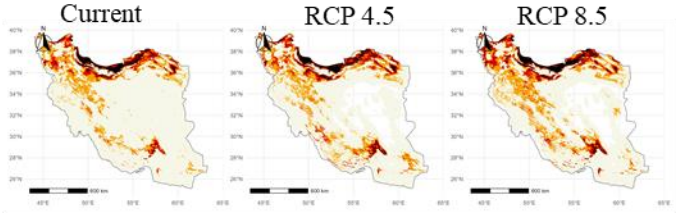

Dalbergia sissoo

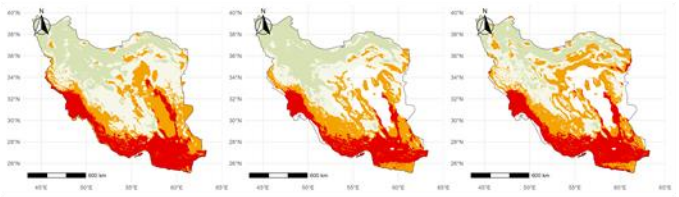

Neltuma juliflora

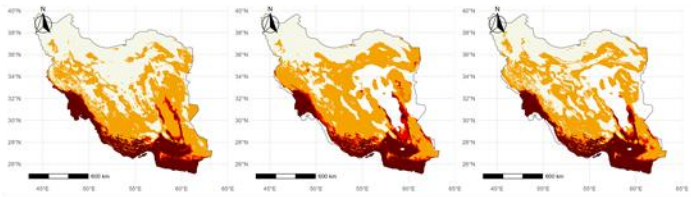

Bambusa vulgaris

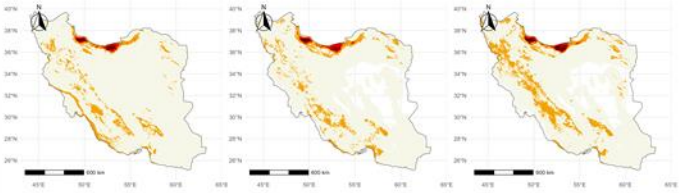

Paulownia fortunei

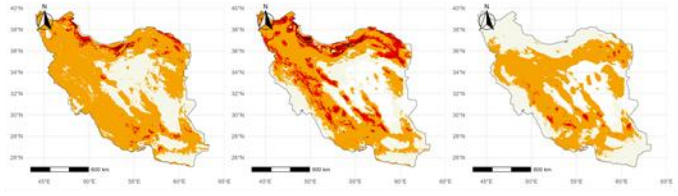

Succulent and halophytic species:

618

Opuntia ficus-indica

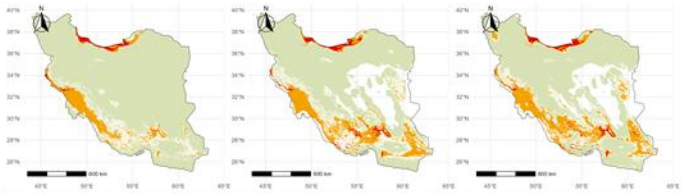

Sesuvium portulacastrum

Aquatic and semi-aquatic taxa:

619

Pistia stratiotes

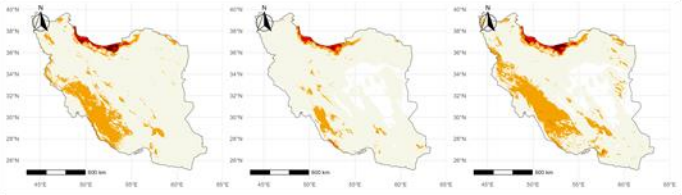

Pontederia crassipes

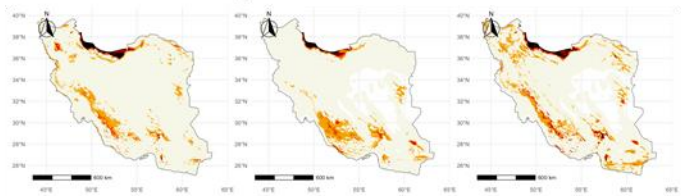

Azolla filiculoides

620

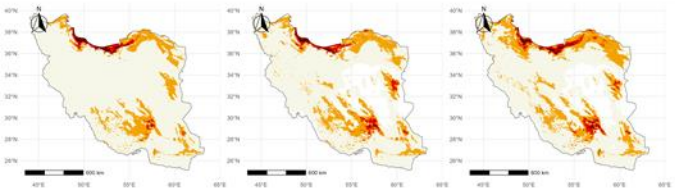

623

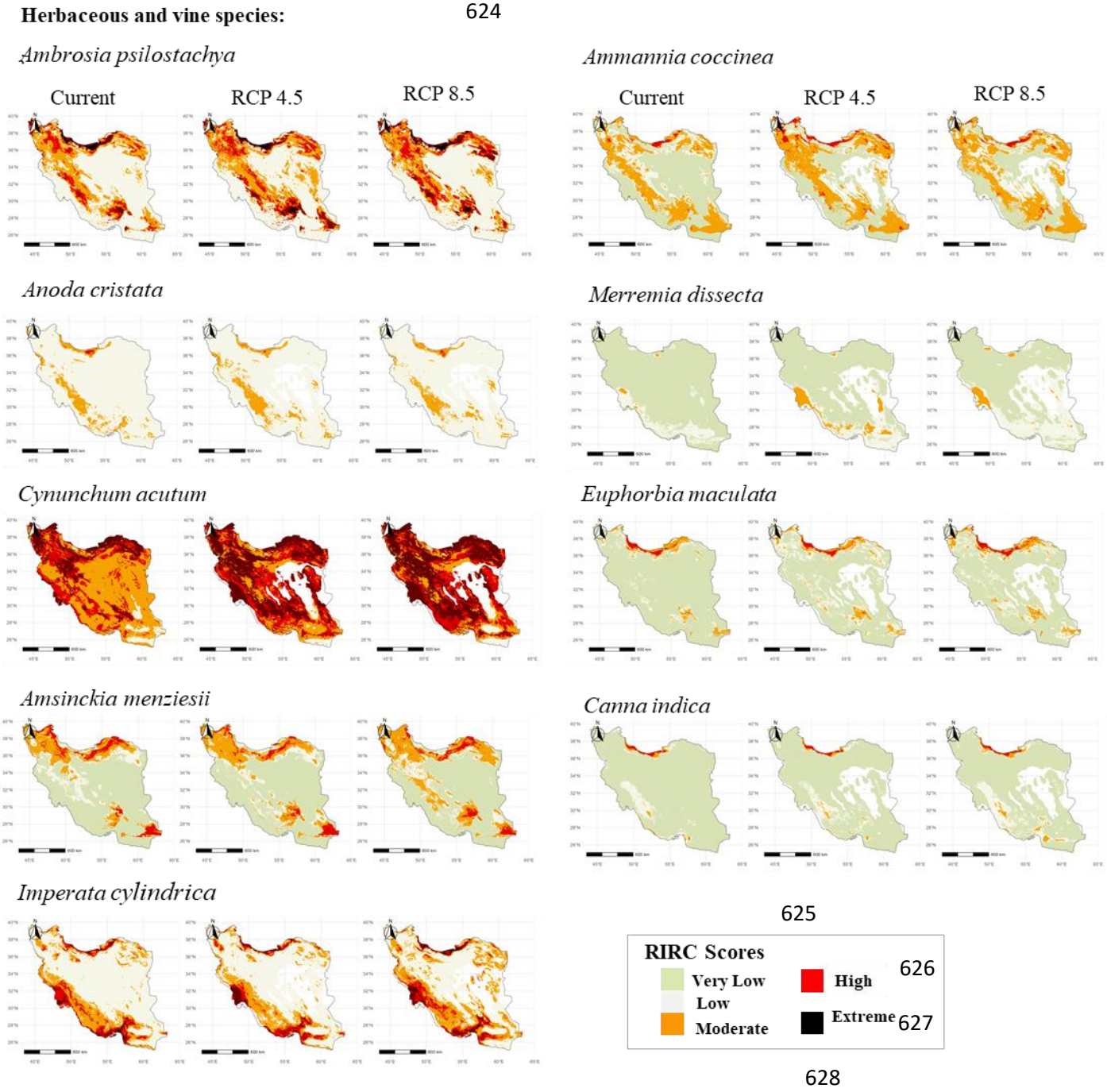

629 **Figure 3.**

630

631

632

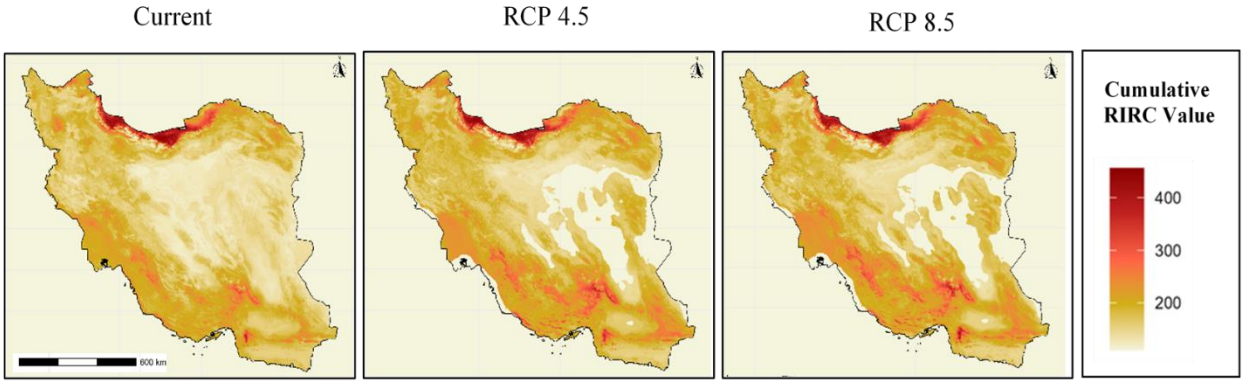
Current
RCP 4.5
RCP 8.5
Cumulative
RIRC Value
400
300
200
600 km

Figure 4.

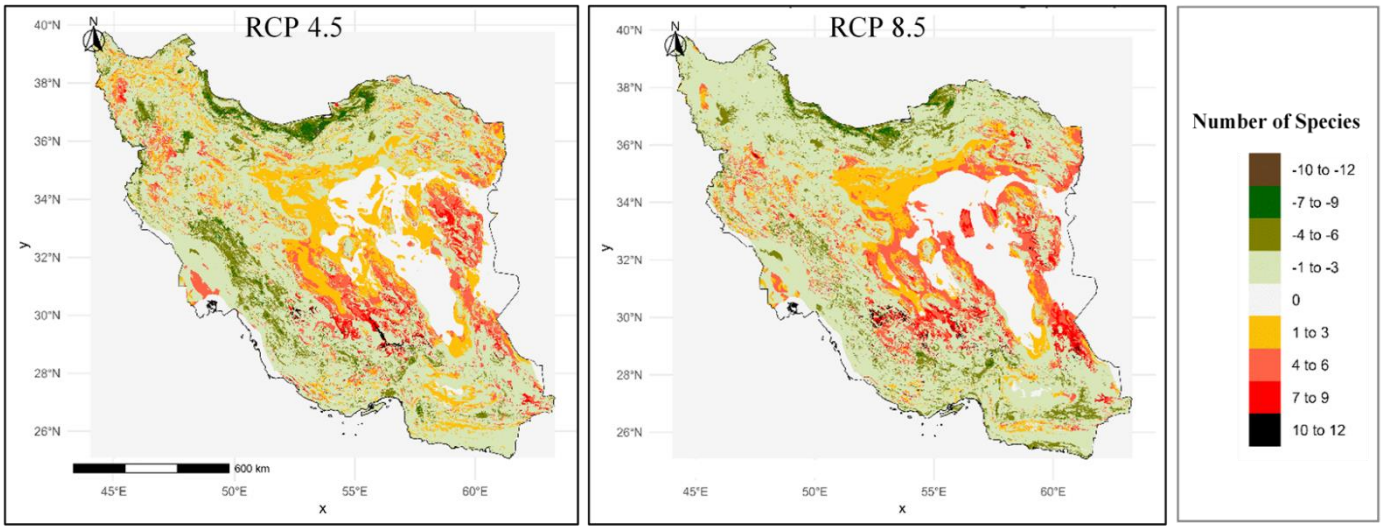
RCP 4.5
RCP 8.5
N
40°N
38°N
36°N
34°N
32°N
30°N
28°N
26°N
45°E
50°E
55°E
60°E
600 km
x
y
Number of Species
-10 to -12
-7 to -9
-4 to -6
-1 to -3
0
1 to 3
4 to 6
7 to 9
10 to 12

Figure 5.

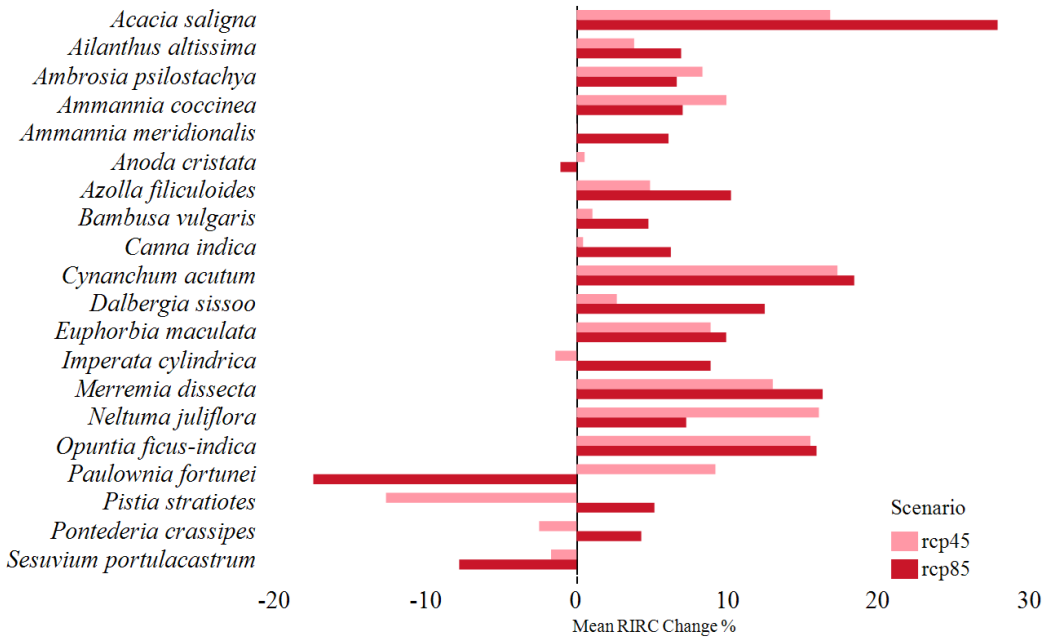
Acacia saligna
Ailanthus altissima
Ambrosia psilostachya
Ammannia coccinea
Ammannia meridionalis
Anoda cristata
Azolla filiculoides
Bambusa vulgaris
Canna indica
Cynanchum acutum
Dalbergia sissoo
Euphorbia maculata
Imperata cylindrica
Merremia dissecta
Neltuma juliflora
Opuntia ficus-indica
Paulownia fortunei
Pistia stratiotes
Pontederia crassipes
Sesuvium portulacastrum
Scenario
rcp45
rcp85
-20
-10
0
10
20
30
Mean RIRC Change %

Figure 6.